# Low Platinum Content Exchange-Coupled CoPt Nanoalloys with Enhanced Magnetic Properties

Georgia Basina *, Vasileios Alexandrakis, Ioannis Panagiotopoulos, Dimitrios Niarchos, Eamonn Devlin, Margarit Gjoka, George C. Hadjipanayis, Vasileios Tzitzios *

Posted Date: 25 October 2023

doi: 10.20944/preprints202310.1606.v1

Keywords: cobalt-platinum alloy; L10 phase; CoPt; Co3Pt; exchange coupling; bimetallic nanoparticles; polyol method

*Article*

# Low Platinum Content Exchange-Coupled CoPt Nanoalloys with Enhanced Magnetic Properties

**Georgia Basina [1,3,*], Vasileios Alexandrakis [1], Ioannis Panagiotopoulos [2], Dimitrios Niarchos [1,5], Eamonn Devlin [1], Margarit Gjoka [1], George C. Hadjipanayis [3,4] and Vasileios Tzitzios [1,*]**

[1] Institute of Nanoscience and Nanotechnology, National Centre for Scientific Research, "Demokritos", 15310, Athens, Greece
[2] Department of Materials Science and Engineering, University of Ioannina, GR, 45110, Ioannina, Greece
[3] Department of Physics and Astronomy, University of Delaware, Newark, DE 19716, USA
[4] Department of Chemical Engineering, Northeastern University, Boston, MA, USA
[5] Amen New Technologies, Athens, Greece
* Correspondence: g.basina@inn.demokritos.gr (G.B.); v.tzitzios@inn.demokritos.gr (V.T.)

**Abstract:** Bimetallic colloidal CoPt nanoalloys, with a very low platinum content, were successfully synthesized following a modified polyol approach. Powder X-ray diffraction, IR spectroscopy, thermogravimetric analysis, and Transmission Electron Microscopy studies were performed to estimate the crystal structure, morphology and surface functionalization of the colloids respectively, while the room temperature magnetic properties were measured using Vibrating Sample Magnetometer. The particles exhibit excellent uniformity, with a narrow size distribution, and display strong room temperature hysteretic ferromagnetic behavior even in the as-made form. Upon annealing at elevated temperatures, progressive formation and co-existence of exchange coupled both chemically ordered and disordered phases, significantly enhance the room temperature coercivity.

**Keywords:** cobalt-platinum alloy; $L1_0$ phase; CoPt; $Co_3Pt$; exchange coupling; bimetallic nanoparticles; polyol method

## 1. Introduction

Magnetic nanoparticles represent one of the most studied classes of nanoparticles because of their size-depended magnetism, especially in the nanoscale regime, and their potential applications in many fields [1–6]. Consequently, a lot of research effort focuses on the development of synthetic methodologies to precisely control their size, shape, composition, crystal structure and surface chemical modification [6–9].

Chemically ordered, bimetallic CoPt nanoparticles are extensively studied due to their technological interest in a variety of fields such as permanent magnets, high density magnetic storage media, catalysis, and biomedicine [10]. The CoPt phase diagram includes several chemically ordered phases as $Co_3Pt$, CoPt and $CoPt_3$ [11,12]. The equiatomic CoPt, when chemically ordered, forms the $L1_0$ high magnetic anisotropy ($K_u$ = 4.9 MJ/m$^3$) tetragonal phase with alternating atomic layers of Co and Pt along the c axis. This phase is reported to exist in the range of 40-60 at. % Platinum composition. The off-equiatomic stoichiometry compositions can be only partially ordered and consequently have somewhat lower anisotropies. On the Pt-rich and the Co-rich sides the $CoPt_3$ and $Co_3Pt$ are formed respectively, which are both chemical ordered cubic $L1_2$ phases and have moderate magnetic anisotropy [13,14].

The high anisotropy values of these CoPt phases [15,16] allow the stabilization of their magnetization against thermal fluctuations and demagnetizing effects at very low dimensions [17–21], properties which are fundamental for application in permanent magnets and recording media [22–25]. Additionally, their chemical stability in alkaline and acidic environments makes them excellent candidates for low platinum content electrocatalysts [26–34].

 doi:10.20944/preprints202310.1606.v1



One of the major commercialization issues still remains the high precious metal content, up to 50 at. %, equivalent to more than 77 wt. %, which is necessary, as previously mentioned, in order to form the chemically ordered $L1_0$ structure. Therefore, there is still a great challenge on the synthesis of CoPt bimetallic alloys, with as low as possible Pt content, maintaining high magnetocrystalline anisotropy, and consequently high coercivity. Previous studies have presented a plethora of chemical routes for the synthesis of ultrafine, monodispersed, bimetallic CoPt nanoparticles [35–41]. The as-made nanoparticles, in the majority of the studies poses the disordered face centered cubic (fcc) crystal structure and shows superparamagnetic behavior. Our group recently published the effect of bismuth addition on the equiatomic CoPt $L1_0$ ordering, in which the particles show partial ordering without any post annealing exhibiting 1.7 kOe room temperature coercivity [42]. In general, thermal treatment at elevated temperatures is required to obtain the fully ordered, magnetically hard, $L1_0$ crystalline phase. The bulk order-disorder transition of CoPt occurs at 825 °C [43], while in the nanosize regime, ordering can take place at temperatures above 650 °C [44,45]. Regarding the synthesis of the $L1_2$ $Co_3Pt$ phase, there are a limited number of works in the literature, and the majority of them are related to synthesis in thin films form [9,46–51]. Here we report the colloidal synthesis of platinum lean CoPt bimetallic nanoalloys following a modified polyol methodology. The materials reveal high uniformity, narrow size distribution and exhibit enhanced room temperature coercivity, up to 14.5 kOe, value which is among the highest in the literature concerning CoPt based nanoalloys of any composition. The enhanced magnetic properties result from the coupling between the magnetically hard $L1_0$, and semi-hard $Co_3Pt$ phases, leading to the formation of an exchange-spring nanocomposite magnetic material.

## 2. Materials and Methods

### *2.1. Materials Synthesis*

Anhydrous $Co(CH_3COO)_2$ and $PtCl_4$ were used as metal precursors, polyethylene glycol 200 (PEG-200) serving as solvent and reducing agent, while oleic acid/oleyl amine utilized as nanoparticles' capping agents. The synthesis was carried out following our previous work [44]. Briefly, a 100 mL spherical flask was charged with a mixture of 20 mL PEG-200, oleic acid/oleyl amine, and the temperature was raised to 100 °C under nitrogen bubbling, followed by the addition of $PtCl_4$ (0.5 mmol), and anhydrous $Co(CH_3COO)_2$ (1.66 mmol) under vigorous magnetic stirring. The reaction was performed at 250-260 °C under $N_2$ mantle. The colloidal particles were precipitated by the addition of ethanol and separated by centrifugation. The excess of oleic acid, oleyl amine, PEG and reaction byproducts, were rinsed by repeated washing with ethanol. Finally, the particles were dried at room temperature under reduced pressure and the reaction yield was estimated gravimetrically. The equiatomic CoPt nanoalloys were synthesized using 0.5 mmol of each metallic precursor following exactly the above methodology.

### *2.2. Materials Characterization*

Powder X-ray diffraction (XRD, Siemens D 500 diffractometer with Cu K$\alpha$ radiation) was performed for the crystal structure analysis and the morphology of the nanoparticles was estimated using transmission electron microscopy (TEM, JEOL JEM-3010). The surface functionalization was estimated by Fourier transform infrared spectroscopy (Bruker FT-IR spectrometer, Equinox 55/S model) while, thermogravimetric analysis, (Perkin-Elmer Pyris Diamond TGA/DTA), took place in order to quantify the organic content. Magnetic measurements were measured at room temperature using vibrating sample magnetometer (VSM) equipped with a 2 T magnet.

## 3. Results and Discussion

The size and the morphology of the platinum lean CoPt nanoalloys in both as-made and extensively annealed (700 °C, 7 h) form were studied by TEM microscopy (Figure 1). The as-made nanoparticles are uniform, and quite monodispersed, while after annealing at 700 °C for 7 h under $H_2$/Ar flow, the particles became slightly irregular without significant sintering and agglomeration.

Preprints (www.preprints.org) | NOT PEER-REVIEWED | Posted: 25 October 2023 doi:10.20944/preprints202310.1606.v1



The as-made particles are well spherically shaped with 7.1 nm mean diameter and narrow size distribution, while the annealed material loses the spherical morphology, and has an average size of 15.7 nm (size distribution histogram is presented in the supplementary material section, Figure S1).

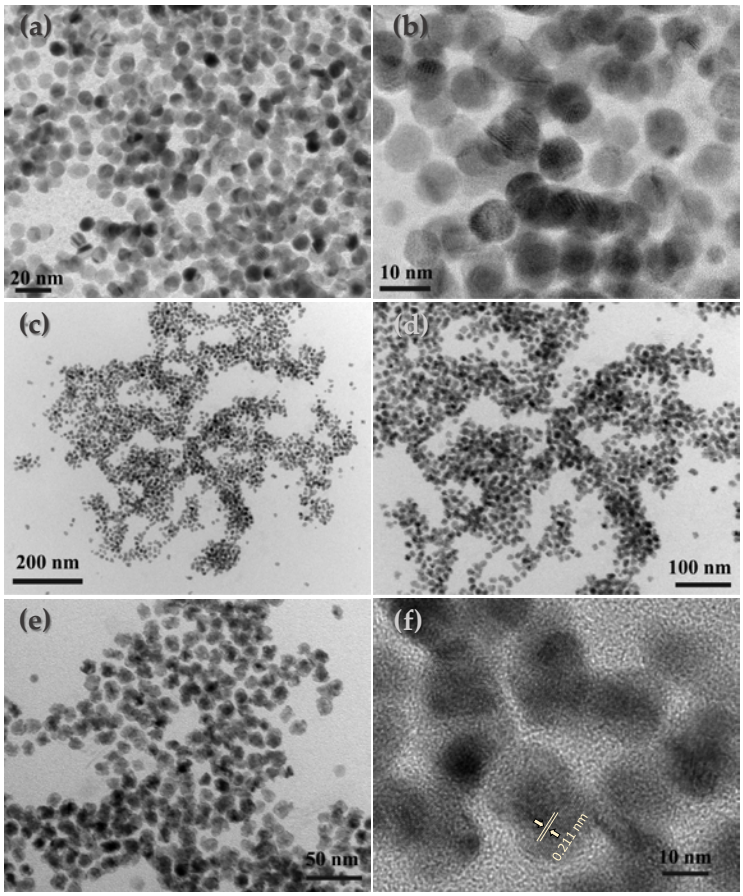


**Figure 1.** TEM and HR-TEM images of the as-made (a, b) and annealed at 700 °C for 7 h under $H_2$-Ar atmosphere (c-f).

Figure 2(a), illustrates the infrared (IR) spectrum of CoPt nanoparticles capped with oleic acid-oleyl amine. The spectrum collected in $CCl_4$ colloidal solution in a liquid cell and shows strong bands at 2854 and 2928 $cm^{-1}$, assignable to the symmetric and asymmetric $CH_2$ stretches of the hydrocarbon moiety respectively; a shoulder at 2960 $cm^{-1}$, due to the asymmetric stretch of the terminal $CH_3$ group and a weak yet definite band at 3006 $cm^{-1}$, which is attributed to the olefinic CH stretch from both oleic acid and oleyl amine molecules. The broad bands around 3400 $cm^{-1}$ are attributed to the $NH_2$ group, confirming the presence of oleyl amine on the nanoparticle surface. Additionally, two other absorptions at 1569 $cm^{-1}$ and 1412 $cm^{-1}$ are characteristic of the presence of carboxylate (-COO-) groups. Moreover, the frequency separation between the bands at 1569 $cm^{-1}$ and 1412 $cm^{-1}$ indicates that the oleate moieties bind the surface atoms in a chelating or bridging mode of coordination. Finally, the band at 1464 $cm^{-1}$ is associated with the $CH_2$ deformation ($\nu_{CH2}$). These data clearly demonstrate the anchoring of both capping agents to the nanoparticles surface. The as-made oleic acid-oleyl amine capped CoPt nanoparticles are easily dispersible in non-polar organic solvents such as hexane, toluene and chloroform with concentration up to several dozen of mg/mL, and are stable for weeks without precipitation. Thermogravimetric analysis was used to determine the mass of the organic matter absorbed on the CoPt nanoparticles (Figure 2(b)). The experiments were carried out under nitrogen atmosphere with 60 mL/min flow and 5 °C/min heating rate. The organic molecules desorption begins around 140-150 °C and the total weight loss is 28 %. At temperatures about 360 – 450 °C the curve approaches an intermediate plateau. This behavior suggests, in agreement with the literature [52], that the weight loss from 140 to 360 °C is due to the desorption of the amine ligand,

Preprints (www.preprints.org) | NOT PEER-REVIEWED | Posted: 25 October 2023 doi:10.20944/preprints202310.1606.v1



and the weight loss above 360 °C is mainly due to the desorption/decomposition of carboxylic residue. The overall desorption procedure completed at approximately 500 °C. The reaction yield was estimated gravimetrically. The dry CoPt powder from a single batch was weighed 254 mg. Considering that 28 wt. % belongs to the organic capping molecules, the net mass of CoPt nanoparticles is 182.9 mg, resulting in a reaction yield of up to 93.6 %. Assuming that the $Pt^{2+}$ reduced quantitative, due to the positive reduction potential (+1.18 V) in contrast with the $Co^{2+}$ (-0.282 V), the estimated nanoalloys atomic composition is $Co_{74.4}Pt_{25.6}$, which is very close to the nominal composition, ($Co_{77}Pt_{23}$), according to the reaction precursors molecular quantities.

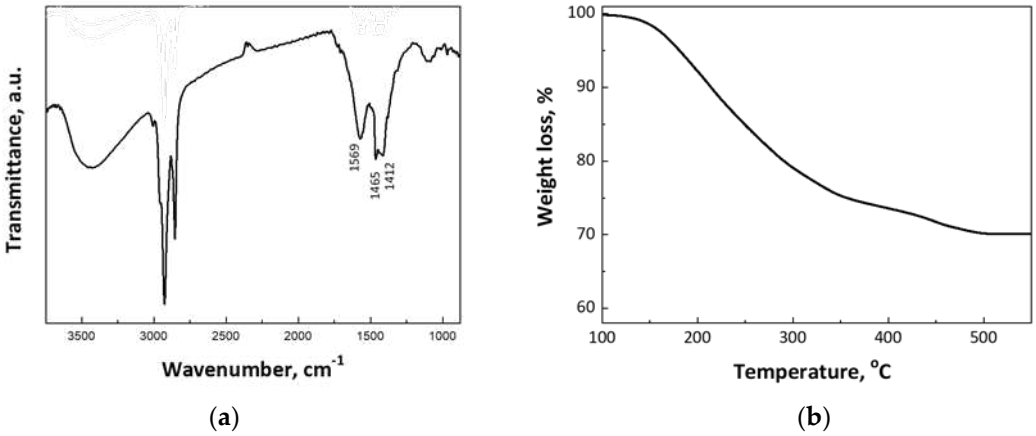


**Figure 2.** FT-IR spectrum (a) and TGA profile (b) from the as-made CoPt bimetallic nanoalloys.

Figure 3(I), shows the powder XRD patterns of the as-made, as well as, the annealed at 700 °C, bimetallic CoPt nanoalloys. The pattern of the as-made material, (Figure 3I(a)), shows clearly that the dominant phase is the chemically disordered fcc. As for the reflection at 2-theta = 31.7° degrees, which remains unmatched and indicated with an asterisk, can be attributed to cobalt oxide phase, probably the $Co_3O_4$ [53]. Furthermore, the broad peaks correspond to a Scherrer structural coherence size of 6 nm in diameter, which is slightly smaller than the particle size which was estimated by the TEM studies (7.1 nm). It is worth to mention that the large unit cell, a=3.88 Å, shows a Pt rich phase [8,54]. This behavior has been previously reported from our group [51], for similar materials, and due to strong compositional gradient from the nanoparticles core to the shell, indicating the presence of a Pt-rich composition at the center of the particle which progressively decrease, and leads to a Co-rich shell and can be explained by the reaction conditions. PEG's, without alkaline environment, as well as, oleyl amine, are mild reducing agents and not able to reduce $Co^{2+}$ to the metallic state [55]. The presence of platinum ions in the reaction, which due to their electropositivity, reduced very easily, without the need of strong reducing agents, leads to the initial formation of tiny Pt seeds, possessing very negative redox potential [56], which consequently can reduce much more easier the $Co^{2+}$ to the metallic state, leading to the formation of particles in which their core is Pt rich [54]. We have also noticed that the chemical ordering requires a short-length scale diffusion process which means that this compositional gradient can be present even if chemical ordering to various phases PtCo-$Pt_{0.4}Co_{0.6}$-$PtCo_3$ (*from center to shell*) has been reached. After thermal treatment at 700 °C for 4 hours, the X-ray diffraction pattern in Figure 3I(b) reveals mixtures of structures consisting of the following phases: A tetragonal phase with a=3.79 Å and c=3.68 Å clearly indicated by the presence of: (001)∽24°, (110)∽33.2°, superlattices, and additionally the presence of (111)∽41.7°, (200)∽47.9° and (002) at 49.3°. The lattice constants of this tetragonal phase are those expected for the stoichiometric fully ordered $L1_0$ CoPt alloy [53,57,58]. On the other hand, the weaker diffraction at 40.5° can be assigned to the (111) of cubic structured CoPt binary alloy. In the case of annealing for longer time, 700 °C for 7h, the shifting and splitting of the main diffractions of the as-made nanoparticles, shows that part of the alloys transformed to the ordered $L1_0$ and cubic $L1_2$ $Co_3Pt$ phases [59,60]. More detailed examination of the powder X-ray diffraction pattern in Figure 3I(c), shows obvious existence of the (001) and (110)

Preprints (www.preprints.org) | NOT PEER-REVIEWED | Posted: 25 October 2023 doi:10.20944/preprints202310.1606.v1



superlattice peaks which clearly indicate the transformation to the chemically ordered tetragonal $L1_0$ phase [54,57,58], while some extra peaks indicate the presence of another phase with weak tetragonality: a=3.73Å and c=3.71Å indicated by the presence of: (111)∽41.88° and (200)∽48.8°, (002)∽49.7°. Since the order parameter S scales with the tetragonicity as $S^2 \backsim$ (1- c/a) the c/a=0.996 compared to the 0.973 of the fully ordered phase gives S=0.37. This could be due to the off-stoichiometric composition of this phase as the lattice parameters are close to what is expected for $Pt_{0.4}Co_{0.6}$. The S of this cobalt-rich phase shows that could reach an anisotropy of 1.8 MJ/m³. Finally, the stronger peaks can be assigned to the cubic $L1_2$ $Co_3Pt$ phase with a=3.66Å: (111) ∽42.6°, (200) ∽49.5°, (220) ∽72.9° and (311) ∽88.4°, and is in agreement with the estimated by HR-TEM images, d-space value (Figure 1(f), 0.211 nm), and assigned with the (111) plane of the $Co_3Pt$ phase, which is also very close to the results reported in the literature [16]. It should be noted that several peaks of the $L1_2$ phase are located very close to those of $L1_0$ making difficult their detection since they are masked each other. According to the phase diagram of bulk CoPt, Co-rich $L1_2$ phase reaches its maximum ordering temperature at around 900 °C, for the optimum stoichiometry and decreases to 700 °C for $Co_{83}Pt_{17}$ [50,57,61,62]. Consequently, increasing annealing time at 700 °C, is expected to increase the proportion of Co-rich $L1_2$ phase. Regarding the crystallite size, obviously, the reflections peaks become sharper and more intensive as the annealing temperature increases. This indicates that the particles size increases with longer annealing times. In particular, the size of the particles derived by the Scherrer equation after annealing at 700 °C for 4 h and 7 h was estimated to 8.8 nm and 17.1 nm, respectively. These values are in good agreement with the sizes estimated from the TEM images.

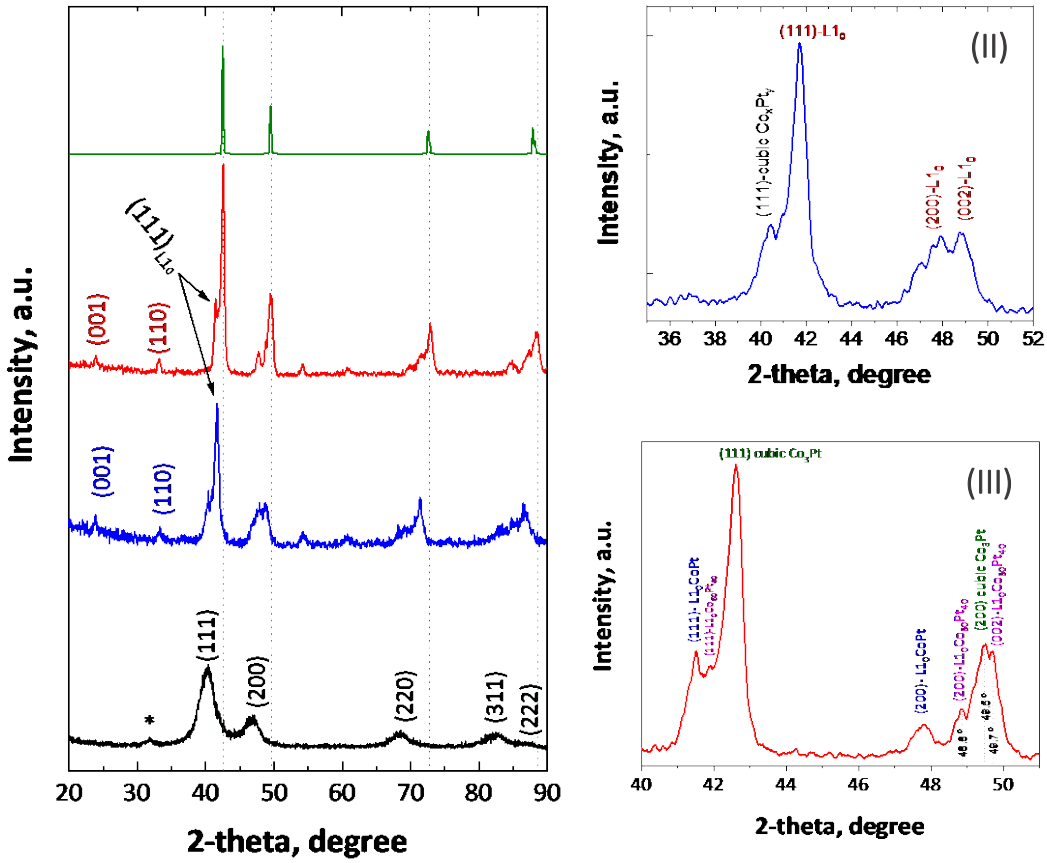


**Figure 3.** XRD patterns of CoPt nanoalloys (I), in the as-made form (a) and after annealing at 700 °C for 4 h (b), 7 h (c) and the calculated $Co_3Pt$ (d). Magnification of XRD patterns of CoPt nanoalloys (II and III), after annealing at 700 °C for 4 (blue line) and 7 (red line) h.

Room temperature magnetic hysteresis loops of CoPt nanoalloys, in the as-made and annealed forms, have been performed in order to study their magnetic properties, and presented in the Figure

Preprints (www.preprints.org) | NOT PEER-REVIEWED | Posted: 25 October 2023 doi:10.20944/preprints202310.1606.v1



4. The as-made CoPt nanoparticles exhibit 59.3 emu/g saturation magnetization, and a moderate coercivity ($H_c$) value, around 1 kOe (Figure 4), which is significantly higher compared to the so-called "soft" magnetic materials where the coercivity is in the range of a few Oe. It is obvious that the as-made CoPt shows hysteretic ferromagnetic behavior which cannot be explained by the structural defects or imperfections (*pinning centers*). Shape anisotropy should also be excluded since the particles are almost perfectly spherical and nearly monodispersed as it turns out from the TEM images. Meanwhile, XRD measurements showed that the as-made nanoalloys consist dominantly of a disordered fcc phase with probably the presence of small amount of cobalt oxide. A possible interpretation should be connected with the presence of compositional gradient in the nanoalloys which is also in agreement with the previously discussion in the XRD section, as well as, the reaction mechanism where the positive (+1.18 volts) $Pt^{2+}$ reduction potential, ensures the initial formation of tiny Pt seeds before the reduction of $Co^{2+}$ ions. Under the regime of such growth mechanism, it is expected that the nanoalloys core would be platinum-rich in contrast with the shell [44]. In the case of annealed nanoalloys it is obvious from the hysteresis loops in Figure 4 that the magnetization value does not correspond to the saturation value, as the 2 T applied field is not sufficient to saturate the magnetization. Therefore, the magnetization, at 2 T magnetic field, is 46.8, 43.6, 36.8, and 33.7 emu/g for the samples after annealing at 700 °C for 30 min, 2, 4, and 7 h respectively. The saturation values were also obtained by fitting the high-field data with the $M=M_S(1-a/H)$ law (Figure S2). Extrapolation gives $M_S$=36.4 emu/g, and therefore $M_R/M_S$= 26.25/36.4=0.72.

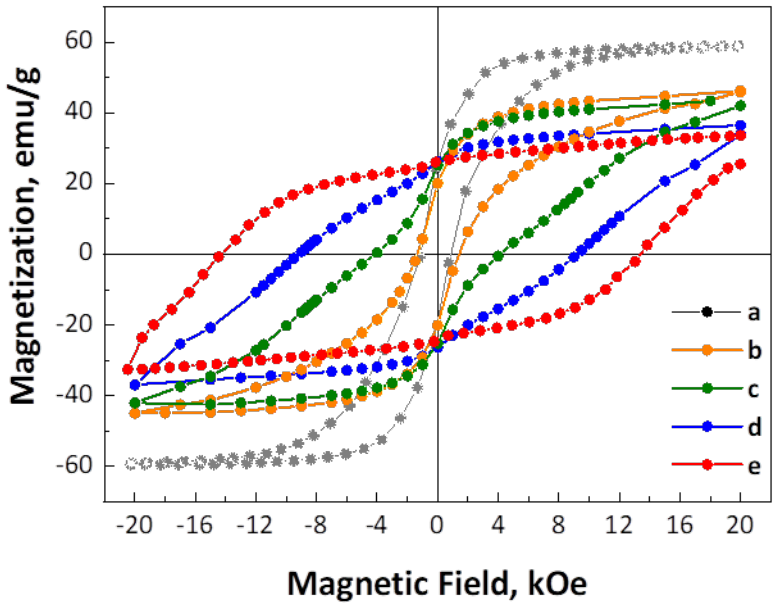


**Figure 4.** Room temperature magnetic hysteresis loops of CoPt nanoalloys in the as-made (a), and after annealing at 700 °C for 30 min (b), 2 (c), 4 (d) and 7 h (e), under mild reductive atmosphere (4 % $H_2$ in Ar).

On the other hand, the room temperature coercivity reached 1.3 4.2, 9.2 and 14.5 kOe, after annealing at 700 °C for 30 min, 2, 4 and 7 h, respectively. Considering the unsaturated magnetization, it is expected that these values will be even higher. By examining the shape of the M vs H curves, it is obvious that there are two different magnetic phases in the materials annealed for shorter times. This behavior becomes less prominent after 4 h annealing, and almost disappears after 7 h annealing. For instance, in the sample annealed for 2 hours, a significant change in the slope of M vs H curve is observed, as indicated by the two local maxima of the derivative (Figure S3). In fact, the two maxima suggest two different magnetization switching mechanisms which correspond to two different magnetic phases with two different coercive fields. This finding is in accordance with the conclusions from the XRD analysis, where different structural phases were identified. Indeed, the present system

 doi:10.20944/preprints202310.1606.v1



of nanoalloys is a mixture of cubic phases with low magnetocrystalline anisotropy, and ordered $L1_0$ tetragonal CoPt phases exhibiting the highest magnetocrystalline anisotropy and coercivity [63]. As the annealing time increases the degree of ordering and the proportion of the $L1_0$ phases increases which results in enhancement of coercivity value. It is evident from the hysteresis loop that, in addition to the increase in coercivity, the M vs H curves become smoother similar to single-phase magnetic hysteresis loops. This behavior it is well known and based on the interactions between magnetically hard and soft phases and described by the exchange-spring magnets theory [64,65]. It has been proven that the higher difference in the magneto-crystalline anisotropy between the two phases the lower should be the thickness (or the proportion) of the soft phase in order to have completely coupled magnetic composite without steps at the demagnetization curve [66]. Therefore, the optimum conditions for effective coupling are more favorable under the presence of phases with intermediate hardness, as in graded stoichiometry nanoparticles. In nanostructured materials that need high temperature annealing is very difficult to precisely control the dimensions of the hard phase and the soft phase in particular [65]. In our case the presence of the $Co_3Pt$ phase, despite being a cubic phase, exhibits a moderate magnetocrystalline anisotropy ($K_u$ = 107 erg/cm$^3$) [15], it appears to be crucial for the formation of a fully exchange coupled spring magnet with a single magnetization switching field ($H_c$) as it's progressive appearance with the annealing time eliminate completely the shoulder in the M vs H curve. The importance of the $Co_3Pt$ phase formation, as well as the off-stoichiometric cobalt rich $L1_0$ phase, is also proved by the magnetic behavior of the nanoalloys when the annealing temperature slightly decreased. After annealing at 675 °C the magnetic hysteresis loops (Figure S4), show that the presence of two different magnetic phases (a soft and a hard), which is much more intense compared to the sample annealed for the same time at 700 °C. The inefficient coupling, may be attributed to the lower $L1_0$ ordering, although we are convinced that it is also linked with the absence of the intermediate magnetocrystalline anisotropy Co-rich phase. Additionally, the remanence to saturation ratio ($M_R/M_S$) is enhanced well above the 0.5 value which is expected for an isotropic sample. This indicates the presence of strong interactions.

Furthermore, it is worth to mention that, by synthesizing equiatomic CoPt nanoalloys, i.e., following the same methodology, but using equimolar cobalt and platinum precursors, shows that after annealing at 700 °C, we obtain a single-phase ferromagnetic material with well crystallized face centered tetragonal phase, ($L1_0$), as presented in the Figure S5, in the supplementary material section.

## 4. Conclusions

Bimetallic CoPt based nanoalloys with low platinum content were successfully synthesized via a facile chemical methodology following a modified polyol process. The nanoparticles in the as-made form are monodispersed with 7.1 nm mean diameter and reveal unexpectedly high room temperature coercive field, up to 1 kOe, which probably originated from the presence of gradients in the nanoalloys composition. After annealing at 700 °C progressively the nanoalloys transformed to the fully and partial ordered $L1_0$ CoPt (hard), and cubic $Co_3Pt$ (semi-hard) correspondingly. The annealed nanoparticles exhibit enhanced room temperature coercive field, up to 14.5 kOe, which is amongst the highest values in the literature and with the lowest platinum content (25 at. %). The formation of the $Co_3Pt$ magnetically semi-hard phase, is very crucial to achieve a fully exchange-spring nanocomposite magnetic material. Therefore, the proposed platinum lean CoPt nanoalloys are very promising candidates for both permanent magnet and electrocatalytic applications.

**Supplementary Material:** The following supporting information can be downloaded at the website of this paper posted on Preprints.org.

**Author Contributions:** The manuscript was written through contributions of all authors. **G.B:** Conceptualization, Investigation, Formal Analysis, writing – original draft. GB performed the materials synthesis and characterization (*TGA, FTIR, VSM*); **V.A:** Methodology, Formal Analysis, V.A. contributed to structural characterization (*XRD*); **I.P:** Investigation, Formal Analysis, writing and editing; **D.N:** Data evaluation – Analysis & Editing; **E.D:** Formal Analysis on structural characterization; **M.G:** Methodology and magnetic measurements; **G.C.H:** Data evaluation, review & editing; **V.T:** Conceptualization, Materials and methodology

design, Writing - review & editing. He is responsible for the overall research work; / All authors have given approval to the final version of the manuscript.

**Funding:** This research received no external funding.

**Conflicts of Interest:** The authors declare no conflict of interest.

## Appendix A

Supplementary data include additional structural, magnetic and morphological characterization results based on XRD, VSM and TEM analysis. Furthermore, selected literature data on the room temperature coercivity values of CoPt-based nanomaterials, are given for comparison (PDF).

## References

1. Krishnan, K.M.; Pakhomov, A.B.; Bao, Y.; Blomqvist, P.; Chun, Y.; Gonzales, M.; Griffin, K.; Ji, X.; Roberts, B.K. Nanomagnetism and spin electronics: materials, microstructure and novel properties. Journal of Materials Science 2006, 41, 793-815.
2. Binns, C. Nanomagnetism: fundamentals and applications; Elsevier: Oxford, England, 2014.
3. Fernández-Pacheco, A.; Streubel, R.; Fruchart, O.; Hertel, R.; Fischer, P.; Cowburn, R.P. Three-dimensional nanomagnetism. Nature Communications 2017, 8, 15756.
4. Abel, F.M.; Tzitzios, V.; Devlin, E.; Alhassan, S.; Sellmyer, D.J.; Hadjipanayis, G.C. Enhancing the Ordering and Coercivity of $L1_0$ FePt Nanostructures with Bismuth Additives for Applications Ranging from Permanent Magnets to Catalysts. ACS Applied Nano Materials 2019, 2, 3146-3153.
5. Liang, J.; Ma, F.; Hwang, S.; Wang, X.; Sokolowski, J.; Li, Q.; Wu, G.; Su, D. Atomic Arrangement Engineering of Metallic Nanocrystals for Energy-Conversion Electrocatalysis. Joule 2019, 3, 956-991.
6. Ali, A.; Shah, T.; Ullah, R.; Zhou, P.; Guo, M.; Ovais, M.; Tan, Z.; Rui, Y. Review on Recent Progress in Magnetic Nanoparticles: Synthesis, Characterization, and Diverse Applications. Frontiers in Chemistry 2021, 9.
7. Singamaneni, S.; Bliznyuk, V.N.; Binek, C.; Tsymbal, E.Y. Magnetic nanoparticles: recent advances in synthesis, self-assembly and applications. Journal of Materials Chemistry 2011, 21, 16819-16845.
8. Wu, L.; Mendoza-Garcia, A.; Li, Q.; Sun, S. Organic Phase Syntheses of Magnetic Nanoparticles and Their Applications. Chemical Reviews 2016, 116, 10473-10512.
9. Andreazza, P.; Pierron-Bohnes, V.; Tournus, F.; Andreazza-Vignolle, C.; Dupuis, V. Structure and order in cobalt/platinum-type nanoalloys: from thin films to supported clusters. Surface Science Reports 2015, 70, 188-258.
10. Zhao, Z.; Fisher, A.; Shen, Y.; Cheng, D. Magnetic Properties of Pt-Based Nanoalloys: A Critical Review. Journal of Cluster Science 2016, 27, 817-843.
11. Okamoto, H. Supplemental Literature Review of Binary Phase Diagrams: Au-La, Ce-Pt, Co-Pt, Cr-S, Cu-Sb, Fe-Ni, Lu-Pd, Ni-S, Pd-Ti, Si-Te, Ta-V, and V-Zn. Journal of Phase Equilibria and Diffusion 2019, 40, 743-756.
12. Kim, D.; Saal, J.E.; Zhou, L.; Shang, S.; Du, Y.; Liu, Z.-K. Thermodynamic modeling of fcc order/disorder transformations in the Co–Pt system. Calphad 2011, 35, 323-330.
13. Lu, X.; Laughlin, D.E.; Zhu, J.-G. On the conditions for ordered hexagonal mm2 $Co_3Pt$. Journal of Magnetism and Magnetic Materials 2019, 491, 165570.
14. Karoui, S.; Amara, H.; Legrand, B.; Ducastelle, F. Magnetism: the driving force of order in CoPt, a first-principles study. Journal of Physics: Condensed Matter 2013, 25, 056005.
15. Yamada, Y.; Suzuki, T.; Kanazawa, H.; Österman, J.C. The origin of the large perpendicular magnetic anisotropy in $Co_3Pt$ alloy thin films. Journal of Applied Physics 1999, 85, 5094-5096.
16. Tokushige, M.; Matsuura, A.; Nishikiori, T.; Ito, Y. Formation of Co–Pt Intermetallic Compound Nanoparticles by Plasma-Induced Cathodic Discharge Electrolysis in a Chloride Melt. Journal of The Electrochemical Society 2011, 158, E21.
17. Skumryev, V.; Stoyanov, S.; Zhang, Y.; Hadjipanayis, G.; Givord, D.; Nogués, J. Beating the superparamagnetic limit with exchange bias. Nature 2003, 423, 850-853.
18. Hasegawa, T.; Long, L.D.; Nakamura, Y. MFM Observation of High Coercivity in Nanostructured Tetragonally Distorted FeCo Films. IEEE Transactions on Magnetics 2021, 57, 1-5.
19. Tzitzios, V.; Basina, G.; Tzitzios, N.; Alexandrakis, V.; Hu, X.; Hadjipanayis, G. Direct liquid phase synthesis of ordered $L1_0$ FePt colloidal particles with high coercivity using an Au nanoparticle seeding approach. New Journal of Chemistry 2016, 40, 10294-10299.
20. Miyashita, E.; Funabashi, N.; Taguchi, R.; Tamaki, T.; Nakamura, S. Dependence of thermal decay on the magnetic cluster size of perpendicular magnetic recording media. Journal of Magnetism and Magnetic Materials 2005, 287, 96-101.

21. Tzitzios, V.; Basina, G.; Gjoka, M.; Boukos, N.; Niarchos, D.; Devlin, E.; Petridis, D. The effect of Mn doping in FePt nanoparticles on the magnetic properties of the $L1_0$ phase. Nanotechnology 2006, 17, 4270.
22. Maat, S.; Marley, A.C. Physics and Design of Hard Disk Drive Magnetic Recording Read Heads. In Handbook of Spintronics, Xu, Y., Awschalom, D.D., Nitta, J., Eds.; Springer Netherlands: Dordrecht, 2016; pp. 977-1028.
23. Christodoulides, J.A.; Huang, Y.; Zhang, Y.; Hadjipanayis, G.C.; Panagiotopoulos, I.; Niarchos, D. CoPt and FePt thin films for high density recording media. Journal of Applied Physics 2000, 87, 6938-6940.
24. Coey, J.M.D. Hard Magnetic Materials: A Perspective. IEEE Transactions on Magnetics 2011, 47, 4671-4681.
25. Advanced Magnetic Nanostructures; Sellmyer, D.; Skomski, R.; Springer US: Boston, MA, 2006.
26. Wang, P.; Shao, Q.; Huang, X. Updating Pt-Based Electrocatalysts for Practical Fuel Cells. Joule 2018, 2, 2514-2516.
27. Wang, S.; Luo, Q.; Zhu, Y.; Tang, S.; Du, Y. Facile Synthesis of Quaternary Structurally Ordered $L1_2$-Pt(Fe, Co, Ni)$_3$ Nanoparticles with Low Content of Platinum as Efficient Oxygen Reduction Reaction Electrocatalysts. ACS Omega 2019, 4, 17894-17902.
28. Ramaswamy, N.; Arruda, T.M.; Wen, W.; Hakim, N.; Saha, M.; Gullá, A.; Mukerjee, S. Enhanced activity and interfacial durability study of ultra low Pt based electrocatalysts prepared by ion beam assisted deposition (IBAD) method. Electrochimica Acta 2009, 54, 6756-6766.
29. Huang, S.; Shan, A.; Wang, R. Low Pt Alloyed Nanostructures for Fuel Cells Catalysts. Catalysts 2018, 8, 538.
30. Wang, Z.; Yao, X.; Kang, Y.; Miao, L.; Xia, D.; Gan, L. Structurally Ordered Low-Pt Intermetallic Electrocatalysts toward Durably High Oxygen Reduction Reaction Activity. Advanced Functional Materials 2019, 29, 1902987.
31. Li, J.; Xi, Z.; Pan, Y.-T.; Spendelow, J.S.; Duchesne, P.N.; Su, D.; Li, Q.; Yu, C.; Yin, Z.; Shen, B.; et al. Fe Stabilization by Intermetallic L10-FePt and Pt Catalysis Enhancement in $L1_0$-FePt/Pt Nanoparticles for Efficient Oxygen Reduction Reaction in Fuel Cells. Journal of the American Chemical Society 2018, 140, 2926-2932.
32. Kongkanand, A.; Gu, W.; Mathias, M.F. Proton-Exchange Membrane Fuel Cells with Low-Pt Content. In Encyclopedia of Sustainability Science and Technology, Meyers, R.A., Ed.; Springer New York: New York, NY, 2017; pp. 1-20.
33. Li, M.; Lei, Y.; Sheng, N.; Ohtsuka, T. Preparation of low-platinum-content platinum–nickel, platinum–cobalt binary alloy and platinum–nickel–cobalt ternary alloy catalysts for oxygen reduction reaction in polymer electrolyte fuel cells. Journal of Power Sources 2015, 294, 420-429.
34. Cao, Y.-Q.; Zi, T.-Q.; Liu, C.; Cui, D.-P.; Wu, D.; Li, A.-D. Co–Pt bimetallic nanoparticles with tunable magnetic and electrocatalytic properties prepared by atomic layer deposition. Chemical Communications 2020, 56, 8675-8678.
35. Demortière, A.; Petit, C. First Synthesis by Liquid−Liquid Phase Transfer of Magnetic $Co_xPt_{100-x}$ Nanoalloys. Langmuir 2007, 23, 8575-8584.
36. Park, J.-I.; Cheon, J. Synthesis of "Solid Solution" and "Core-Shell" Type Cobalt−Platinum Magnetic Nanoparticles via Transmetalation Reactions. Journal of the American Chemical Society 2001, 123, 5743-5746.
37. Ely, T.O.; Pan, C.; Amiens, C.; Chaudret, B.; Dassenoy, F.; Lecante, P.; Casanove, M.J.; Mosset, A.; Respaud, M.; Broto, J.M. Nanoscale Bimetallic CoxPt1-x Particles Dispersed in Poly(vinylpyrrolidone): Synthesis from Organometallic Precursors and Characterization. The Journal of Physical Chemistry B 2000, 104, 695-702.
38. Chen, M.; Nikles, D.E. Synthesis, Self-Assembly, and Magnetic Properties of $Fe_xCo_yPt_{100-x-y}$ Nanoparticles. Nano Letters 2002, 2, 211-214.
39. Bian, B.; He, J.; Du, J.; Xia, W.; Zhang, J.; Liu, J.P.; Li, W.; Hu, C.; Yan, A. Growth mechanism and magnetic properties of monodisperse $L1_0$-Co(Fe)Pt@C core–shell nanoparticles by one-step solid-phase synthesis. Nanoscale 2015, 7, 975-980.
40. Li, J.; Sharma, S.; Wei, K.; Chen, Z.; Morris, D.; Lin, H.; Zeng, C.; Chi, M.; Yin, Z.; Muzzio, M.; et al. Anisotropic Strain Tuning of $L1_0$ Ternary Nanoparticles for Oxygen Reduction. Journal of the American Chemical Society 2020, 142, 19209-19216.
41. Karmaoui, M.; Amaral, J.S.; Lajaunie, L.; Puliyalil, H.; Tobaldi, D.M.; Pullar, R.C.; Labrincha, J.A.; Arenal, R.; Cvelbar, U. Smallest Bimetallic $CoPt_3$ Superparamagnetic Nanoparticles. The Journal of Physical Chemistry Letters 2016, 7, 4039-4046.
42. Abel, F.M.; Basina, G.; Tzitzios, V.; Alhassan, S.M.; Sellmyer, D.J.; Hadjipanayis, G.C. Ferromagnetic $L1_0$-Structured CoPt Nanoparticles for Permanent Magnets and Low Pt-Based Catalysts. ACS Applied Nano Materials 2021, 4, 9231-9240.
43. Le Bouar, Y.; Loiseau, A.; Finel, A. Origin of the complex wetting behavior in Co-Pt alloys. Physical Review B 2003, 68, 224203.

44. Tzitzios, V.; Niarchos, D.; Margariti, G.; Fidler, J.; Petridis, D. Synthesis of CoPt nanoparticles by a modified polyol method: characterization and magnetic properties. Nanotechnology 2005, 16, 287.
45. Wellons, M.S.; Gai, Z.; Shen, J.; Bentley, J.; Wittig, J.E.; Lukehart, C.M. Synthesis of $L1_0$ ferromagnetic CoPt nanopowders using a single-source molecular precursor and water-soluble support. Journal of Materials Chemistry C 2013, 1, 5976-5980.
46. Wang, Y.; Zhang, X.; Liu, Y.; Jiang, Y.; Zhang, Y.; Wang, J.; Liu, Y.; Liu, H.; Sun, Y.; S D Beach, G.; et al. Fabrication, structure and magnetic properties of $CoPt_3$, CoPt and $Co_3Pt$ nanoparticles. Journal of Physics D: Applied Physics 2012, 45, 485001.
47. Min, J.H.; Wu, J.H.; Cho, J.U.; Lee, J.H.; Ko, Y.-D.; Liu, H.-L.; Chung, J.-S.; Kim, Y.K. Electrochemical preparation of $Co_3Pt$ nanowires. physica status solidi (a) 2007, 204, 4158-4161.
48. Chen, H.M.; Hsin, C.F.; Chen, P.Y.; Liu, R.-S.; Hu, S.-F.; Huang, C.-Y.; Lee, J.-F.; Jang, L.-Y. Ferromagnetic $CoPt_3$ Nanowires: Structural Evolution from fcc to Ordered L12. Journal of the American Chemical Society 2009, 131, 15794-15801.
49. Sirtori, V.; Cavallotti, P.L.; Rognoni, R.; Xu, X.; Zangari, G.; Fratesi, G.; Trioni, M.I.; Bernasconi, M. Unusually Large Magnetic Anisotropy in Electrochemically Deposited Co-Rich Co–Pt Films. ACS Applied Materials & Interfaces 2011, 3, 1800-1803.
50. Maret, M.; Cadeville, M.C.; Staiger, W.; Beaurepaire, E.; Poinsot, R.; Herr, A. Perpendicular magnetic anisotropy in $Co_xPt_{1-x}$ alloy films. Thin Solid Films 1996, 275, 224-227.
51. Maret, M.; Cadeville, M.C.; Herr, A.; Poinsot, R.; Beaurepaire, E.; Lefebvre, S.; Bessière, M. Enhanced perpendicular magnetic anisotropy in chemically long-range ordered (0001) $Co_xPt_{1-x}$ films. Journal of Magnetism and Magnetic Materials 1999, 191, 61-71.
52. Radychev, N.; Lokteva, I.; Witt, F.; Kolny-Olesiak, J.; Borchert, H.; Parisi, J. Physical Origin of the Impact of Different Nanocrystal Surface Modifications on the Performance of CdSe/$P_3$HT Hybrid Solar Cells. The Journal of Physical Chemistry C 2011, 115, 14111-14122.
53. He, T.; Chen, D.; Jiao, X. Controlled Synthesis of $Co_3O_4$ Nanoparticles through Oriented Aggregation. Chemistry of Materials 2004, 16, 737-743.
54. Tzitzios, V.; Niarchos, D.; Gjoka, M.; Boukos, N.; Petridis, D. Synthesis and Characterization of 3D CoPt Nanostructures. Journal of the American Chemical Society 2005, 127, 13756-13757.
55. Panagiotopoulos, I.; Alexandrakis, V.; Basina, G.; Pal, S.; Srikanth, H.; Niarchos, D.; Hadjipanayis, G.; Tzitzios, V. Synthesis and Magnetic Properties of Pure Cubic CoO Nanocrystals and Nanoaggregates. Crystal Growth & Design 2009, 9, 3353-3358.
56. Henglein, A. Small-particle research: physicochemical properties of extremely small colloidal metal and semiconductor particles. Chemical Reviews 1989, 89, 1861-1873.
57. Xiao, Q.F.; Brück, E.; Zhang, Z.D.; de Boer, F.R.; Buschow, K.H.J. Phase transformation and magnetic properties of bulk CoPt alloy. Journal of Alloys and Compounds 2004, 364, 64-71.
58. Xia, G.; Wang, S.; Jeong, S.-J. A universal approach for template-directed assembly of ultrahigh density magnetic nanodot arrays. Nanotechnology 2010, 21, 485302.
59. Ohtake, M.; Suzuki, D.; Futamoto, M. Characterization of metastable crystal structure for Co-Pt alloy thin film by x-ray diffraction. Journal of Applied Physics 2014, 115.
60. Mourdikoudis, S.; Simeonidis, K.; Gloystein, K.; Angelakeris, M.; Dendrinou-Samara, C.; Tsiaoussis, I.; Kalogirou, O. Tailoring the morphology of CoxPt1−x magnetic nanostructures. Journal of Magnetism and Magnetic Materials 2009, 321, 3120-3125.
61. Sanchez, J.M.; Mora◉-Lopez, J.L.; Leroux, C.; Cadeville, M.C. CHEMICAL AND MAGNETIC ORDERING IN CoPt. J. Phys. Colloques 1988, 49, C8-107-C108-108.
62. Leroux, C.; Cadeville, M.C.; Pierron-Bohnes, V.; Inden, G.; Hinz, F. Comparative investigation of structural and transport properties of L10 NiPt and CoPt phases; the role of magnetism. Journal of Physics F: Metal Physics 1988, 18, 2033.
63. Hadjipanayis, G.; Gaunt, P. An electron microscope study of the structure and morphology of a magnetically hard PtCo alloy. Journal of Applied Physics 2008, 50, 2358-2360.
64. Skomski, R.; Coey, J.M.D. Giant energy product in nanostructured two-phase magnets. Physical Review B 1993, 48, 15812-15816.
65. Zeng, H.; Li, J.; Liu, J.P.; Wang, Z.L.; Sun, S. Exchange-coupled nanocomposite magnets by nanoparticle self-assembly. Nature 2002, 420, 395-398.
66. Chakka, V.M.; Shan, Z.S.; Liu, J.P. Effect of coupling strength on magnetic properties of exchange spring magnets. Journal of Applied Physics 2003, 94, 6673-6677.